

# The effect of noise fluctuation of a quantum tunneling device coupled to a substrate

Nikhilesh A. Vaidya

*Department of Physics, Temple University, Philadelphia, PA 19122, USA*

D. H. Santamore

*Department of Physics and Engineering Physics,  
Delaware State University, Dover, DE 19901, USA*

(Dated: September 11, 2021)

The recent experiment of Stettenheim, et al. showed that, contrary to conventional belief, the coupling of a quantum electronic device to its substrate can have important effects on the noise power spectrum, since the substrate functions as a mechanical oscillator. We carry out a theoretical analysis of this coupling in the case of a quantum point contact (QPC). First we derive the noise power spectrum from the Hamiltonian without making the Markovian approximation, and obtain numerical results that reproduce the experimental data. Next we investigate the nature of the coupling. In most previous analyses, the coupling of an electronic device to a mechanical oscillator has been modeled as a position coupling. We model it both as a position coupling and as a momentum coupling and compare the results. We find that, as long as one includes backaction between position and momentum, the assumed mode of coupling makes little difference, since the backaction transmits momentum fluctuations to position fluctuations and vice versa. Finally, we ask whether the salient features of the model persist in the Markovian approximation. We find that a Markovian analysis confirms the QPC-substrate coupling, but underestimates the noise floor and leads to excessively sharp and narrow noise peaks around the resonant frequencies.

PACS numbers: 73.23.Hk, 74.78.Na, 72.10.-d, 05.40.-a

Keywords: Backaction, Quantum Noise, Fluctuations, Spectral Density, Quantum Point Contact, Nanoelectromechanical systems, Electron transport

## I. INTRODUCTION

In recent years, there has been rapid progress in developing new electronic devices, in which electrical and mechanical degrees of freedom are coupled<sup>1-11</sup>. Electron tunneling devices are especially interesting, since they exhibit a fascinating interplay between macroscopic and mesoscopic phenomena, opening up new avenues in the study of high precision measurement<sup>12-19</sup>. The leading candidates for ultra-precision motion and mass sensors include quantum dots, single electron transistors, and quantum point contacts (QPCs)<sup>20</sup>.

All devices are built on substrates that provide them with a sturdy and compact platform, yet hardly any attention has been given to the substrates: as they are not considered the interesting parts of the system, they have been ignored in most analyses. However, a recent experiment by Stettenheim et al.<sup>2</sup> revealed a surprising fact: some electronic devices are naturally coupled to their substrates, which function as mechanical oscillators. In their experiment, the device-substrate coupling is seen in the power noise spectrum: the fundamental harmonics of the substrate resonant bending mode frequency,  $f_b$ , appeared in the noise spectrum as two spikes  $\pm f_b$  away from the device circuit resonant frequency. This noise can reduce the device's sensitivity by decreasing the coherence between the sample and the device coupling. Since all electronic devices are necessarily built on substrates, this type of coupling is unavoidable. Therefore, it is essential to understand the device-substrate coupling mechanism and its effects.

We investigate the coupling mechanism of an electron tunneling device with its substrate. To demonstrate clearly the effects of substrates, we analyze a specific type of electronic device – a QPC – since experimental noise data for QPCs are publicly available. This paper has three objectives. (1) We introduce a model that faithfully reproduces the experimental result of Ref.<sup>2</sup>, (2) We resolve a long-standing issue concerning the nature of the coupling between an electronic device and a mechanical oscillator: is it a position coupling or a momentum coupling? Most previous work has assumed that the coupling is a position coupling, but we show that, under certain conditions, the assumption of momentum coupling gives equally good results. (3) We examine the applicability of the Markovian approximation that is frequently used for electronic device analyses.

In connection with the first objective, there have been some previous attempts to reproduce the noise spectrum<sup>21</sup>. These studies have successfully reproduced the location of the fundamental harmonic peaks around the circuit resonant frequency, but they do not capture the magnitude of the peaks and the noise floor seen in the experimental data. Our model improves on these previous work by incorporating backaction, evaluating the dynamics without relying on the Markovian approximation, and utilizing parallel computing. We derive the quantum master equation from the Hamiltonian. Then we calculate the correlations between the oscillator and the detector, analytically derive the transport properties of the current, and numerically evaluate the noise spectrum, which we then compare with the experiment of

Stettenheim et al.<sup>2</sup>

Our second and third objectives have to do with the validity and applicability of some common assumptions made in modeling electronic devices involving mechanical oscillators: (a) that the coupling between the system and a mechanical oscillator is mediated by position, (b) that the Markovian approximation on the reservoirs is justified.

The coupling between an electronic device and a mechanical oscillator is commonly assumed to be a position coupling, with only a few researchers positing a momentum coupling. However, there haven't been no firm evidence as to which coupling assumption is appropriate or whether both are valid. Note that we are concerned with harmonic coupling only for a position coupling. Anharmonic coupling either does not exist or is negligible in this context. We address this long-standing puzzle in terms of fluctuation noise. We examine the two coupling assumptions separately, and calculate the dynamics and noise spectrum for each coupling. We show that backaction is the key to the coupling argument. In position coupling, momentum “kicks back” electrons that tunnel through the junction, which then transmit back the “kick” effect to the oscillator position, creating a feedback loop between position and momentum. In momentum coupling, the roles of position and momentum are exactly reversed. As a result, once a feedback loop is established, both position and momentum fluctuations equally affects the system through backaction regardless of which coupling one starts with. We argue that as long as one includes the backaction, the type of coupling does not materially affect the system's steady-state noise spectrum.

Finally, we examine whether the Markovian approximation is sufficient to capture all the crucial features in the noise spectrum. We analytically solve and evaluate the dynamics in the Markovian approximation, and then compare the results with those obtained from full non-Markovian calculations. We show that the Markovian approximation can capture the oscillator's fundamental bending mode coupling signature of noise peaks at the oscillator resonance frequency, but substantially underestimates the noise floor and predicts sharper noise peaks than those seen in the full numerical non-Markovian model.

## II. MODEL AND DERIVATIONS

Our model consists of a QPC and a substrate that acts as a mechanical oscillator. We choose a QPC as our representative electron tunneling device for the sake of definiteness and clarity, and to compare the noise spectrum with that of the experiment in Ref.<sup>2</sup>. However, our method can be applied to any tunneling junction device. The QPC has two fermionic reservoirs, noted as left (L) and right (R). We assume that the tunneling electrons couple to the substrate oscillator's fundamental bending mode by position coupling. Figure 1 shows a schematic

of our model. The Hamiltonian of the system is

$$H_{tot} = H_{osc} + H_{res} + H_{int}, \quad (1)$$

where  $H_{osc}$  and  $H_{res}$  are the non-interacting Hamiltonians for the substrate and the electron reservoirs,

$$H_{osc} = \frac{p^2}{2M} + \frac{1}{2}M\omega_0^2x^2, \quad (2)$$

$$H_{res} = \sum_k \left( \varepsilon_{L,k} a_{L,k}^\dagger a_{L,k} + \varepsilon_{R,k} a_{R,k}^\dagger a_{R,k} \right). \quad (3)$$

Here,  $\omega_0$  is the oscillator resonant frequency,  $M$  is the mass of the substrate oscillator and  $x$  and  $p$  are the position and momentum operators of the oscillator,  $\varepsilon_{L(R),k}$  is the energy of the electrons in the left (right) reservoir with momentum  $k$ , and  $a$  ( $a^\dagger$ ) is the electron annihilation (creation) operator.

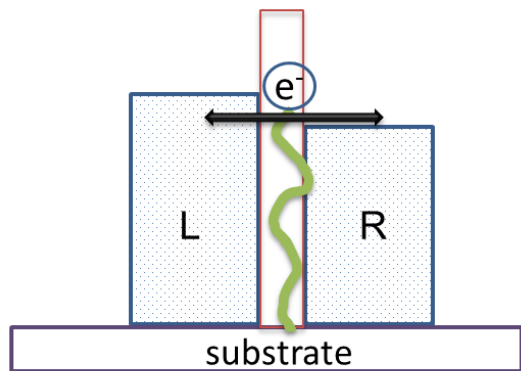


FIG. 1: Schematics of the model. Two reservoirs (right and left) are separated by a barrier. The whole system is built on a substrate that acts as a mechanical oscillator. The oscillator's bending mode is coupled to the tunneling electrons. A bias is applied to cause electrons to tunnel from the left reservoir to the right reservoir (forward bias).

The interaction Hamiltonian  $H_{int}$  describes the tunneling electrons that are coupled to the substrate, and is given by

$$H_{int} = T(x; t) \sum_{k,q} Y^\dagger a_{R,k}^\dagger a_{L,q} + H.c., \quad (4)$$

where  $T(x; t)$  is the electron tunneling amplitude matrix, which depends on the oscillator's position and includes the backaction, the density of states of electrons in the reservoirs, tunnelling amplitude coefficients for with and without the oscillator coupling, and the phase difference between the non-coupled and coupled tunneling amplitudes<sup>22</sup>. To obtain the charge transport and the charge transfer statistics, we employ a charge counting method originally developed by Shelankov and Rammer<sup>17,23-25</sup>. This method extracts particle transfer

information directly from the wave function of a many-body system. The charge counting operators  $\hat{Y}$ ,  $\hat{Y}^\dagger$  are dimensionless and contain charge projection operators that project the state of the conduction electrons onto the density matrix of the electrons. These operators count the number of electron that have tunneled from the left reservoir to the right reservoir. Details of the method and the full expression of  $T(x; t)$  and  $\hat{Y}$  are in Appx. A.

The total density matrix  $\rho_{tot}$  contains all information about the system and the oscillator and their interactions. The oscillator density matrix  $\rho_{osc}$  evolution is described by the equation of motion

$$\frac{d}{dt}\rho_{osc}(t) = \frac{1}{i\hbar} [H_{tot}(t), \rho_{tot}(t)]. \quad (5)$$

We assume that (a) the coupling between the oscillator and the tunneling electrons is weak, and (b) the density matrices  $\rho_{osc}$  and  $\rho_{res}$  of the oscillator and the electron reservoirs are initially uncorrelated,  $\rho(t=0) = \rho_{osc}(t=0) \otimes \rho_{res}(t=0)$ . Then, we can use the Born approximation to obtain the reduced master equation of the oscillator

$$\begin{aligned} \frac{d}{dt}\rho_{osc}(t) = & -\frac{1}{\hbar^2} \int_0^t dt' \\ & \times \text{Tr}_{res} [H_{int}(t), [H_{int}(t'), \rho_{osc}(t) \otimes \rho_{res}]]. \end{aligned} \quad (6)$$

To solve the master equation and find the noise spectrum, we take a similar approach to that of Doiron<sup>26</sup> and calculate an equation of motion for the oscillator's  $n$ -resolved density matrix. We do not adopt the Markovian approximation or any other simplifications. The Markovian approximation is useful when the two-time correlations of the reservoir decay much faster than the coherence time between the QPC and the substrate oscillator in the system, so that we can substitute  $\rho_{osc}(t, t') \rightarrow \rho_{osc}(t)$  and replace the upper time limit  $t$  in the integral by  $\infty$ <sup>27</sup>. However, since we do not know the rate of the correlation decay beforehand, we perform the un-assumed, full numerical integration, and then, compare the results with those obtained in the Markovian approximation. We show in Sec. III C that the Markovian approximation misses some important features of the noise spectrum.

From Eq. (6), we obtain the number-resolved ( $n$ -resolved) master equation

$$\frac{d}{dt}\rho_{osc}(n, t) = -\frac{1}{\hbar^2} \sum_{k, q} \frac{1}{\Lambda} \int_0^t dt' [U(n) + V(n)]. \quad (7)$$

Here  $n$  is the number of charges transferred,  $\Lambda$  is the density of states for the electrons in the reservoirs originally in the tunneling amplitude matrix  $T$ , and  $U(n) + V(n)$  contains the tunneling counting information and the two-time reservoir correlation functions, and also depends on the energy of tunneling junction of the QPC (see Appx. A for details.) Directly solving Eq. (7) for all  $n$  is numerically impractical as  $n$  tends to be large. To get

around this computational problem, we introduce the counting field  $\chi$  to change the sum of number  $n$  to a field  $\rho_{osc}(\chi; t) = \sum_n e^{i\chi n} \rho_{osc}(n; t)$  that describes charge transfer events. After some manipulations, we obtain the unconditional master equation

$$\frac{d}{dt}\rho_{osc}(t) = \varrho_0(\chi=0, t) + \varrho_1(\chi, t), \quad (8)$$

where  $\varrho_0$  and  $\varrho_1$  contain all correlations and transport properties (c.f. Appx. A).

We can now calculate the transport properties for the forward bias regime. The average current is given by  $\langle I(t) \rangle = (2e) d \langle n(t) \rangle / dt$ , where  $e$  is the electron charge,  $n$  is the number of transferred electrons across the junction at time  $t$ , and  $\langle n \rangle$  is given by

$$\frac{d}{dt} \langle n(t) \rangle = i \text{Tr}_{osc} \left[ \frac{d}{d\chi} \left( \frac{d}{dt} \rho_{osc}(\chi; t) \right) \right]_{\chi=0}, \quad (9)$$

with  $d\rho_{osc}/dt$  is given by Eq. (8). We first take the derivative of Eq. (9) with respect to the counting field conjugate to the transferred charge  $n$ . Performing the calculations and simplifying, we obtain

$$\frac{\langle I(t) \rangle}{2e} = \frac{1}{2e} \left( \langle I \rangle_0 + \langle I \rangle_x + \langle I \rangle_p + \langle I \rangle_{xp} + \langle I \rangle_q \right). \quad (10)$$

Here  $\langle I \rangle_0$  is the current without the oscillator coupling,  $\langle I \rangle_x$  and  $\langle I \rangle_p$  are the currents modulated by the coupled oscillator through the oscillator's position and through momentum,  $\langle I \rangle_{xp}$  contains the backaction channel that connects position and momentum, and  $\langle I \rangle_q$  is the quantum correction to the overall current. The analytical expressions of each term are in Appx. B 1.

Next we determine the spectral density  $S(\omega)$  of the current by calculating the variance of  $n(t)$ . The current noise spectrum is given by

$$S(\omega) = \int_{-\infty}^{\infty} dt e^{i\omega t} \langle \{\delta I(t), \delta I(0)\} \rangle, \quad (11)$$

where  $\delta I$  is the fluctuation of the current. A coupled system eventually loses its coherence through interactions with the environment. If the coherence time of the QPC and the substrate oscillator is longer than the decay time of the correlation function of the electrons in the right and left reservoirs, then one can use the MacDonald formula to analytically calculate the spectral density<sup>28</sup>. However, if the reservoir electron's correlation decays much more slowly, the MacDonald formula is not applicable. We perform a full numerical evaluation of the modified spectral density<sup>29</sup> given by

$$\langle S(\omega) \rangle = 2e^2 \omega \int_0^{t'} dt e^{i\omega t} \frac{d}{dt} \langle \langle n^2(t) \rangle \rangle, \quad (12)$$

where  $\langle \langle \cdot \rangle \rangle$  denotes covariance and  $\langle \langle n^2(t) \rangle \rangle$  is obtained by

$$\frac{d}{dt} \langle \langle n^2(t) \rangle \rangle = \frac{d}{dt} \langle n^2(t) \rangle - 2 \langle n(t) \rangle \frac{d}{dt} \langle n(t) \rangle. \quad (13)$$

All higher moments and the correlations between the oscillator and the transferred charge  $n$  are calculated from Eqs. (8) and (A41). Performing the calculations and simplifying, we obtain

$$\frac{d}{dt} \langle \langle n^2(t) \rangle \rangle = \frac{d}{dt} \langle n(t) \rangle + \tilde{N}_x(x, t) + \tilde{N}_p(p, t) + \tilde{N}_{xp}(x, p, t), \quad (14)$$

where  $\tilde{N}_x(x, t)$ ,  $\tilde{N}_p(p, t)$ , and  $\tilde{N}_{xp}(x, p, t)$  are expressions for the noise associated with the correlations  $\langle \langle xn \rangle \rangle$ ,  $\langle \langle pn \rangle \rangle$ , and  $\langle \langle \{x, p\} n \rangle \rangle$ , respectively as well as with their higher moments. The details of these terms are in Appx. B 2. Solving the differential equations for the correlations turns out to be very computationally demanding. Therefore, we use the double exponential oscillatory method developed by Takahasi and Mori<sup>30</sup>, in which the variable  $\omega$  is transformed and the trapezoidal rule is used to solve the transformed integral instead of the original integral<sup>31</sup>.

### III. RESULTS AND DISCUSSION

#### A. Comparison of theory and experiment

In this section, noise power spectrum  $S(\omega)$  is converted to  $P_n$  (dBm) to compare to the experimental results in Ref.<sup>2</sup> by first calculate  $P_n(W)$  in Watts:

$$P_n(W) = S(\omega) e^2 \omega_0 \left( \frac{2L}{CZ} \right) B_W \quad (15)$$

and then, converted to a millidecibel scale. Here  $C = 0.28$  pF is the capacitance and  $L = 140$  nH is the inductance, and  $Z = 50$  is the impedance of the LC tank circuit.  $B_w$  is the bandwidth from the measurement.

Figure 2 shows the noise power spectrum  $P_n$  as a function of the dimensionless frequency  $\tilde{\omega}$ , with the parameters used in the experiments in Ref.<sup>2</sup>. In the experiment, the QPC was embedded in an LC tank circuit. The resonant frequency of the LC circuit was  $f_0 = 800$  MHz, the electron reservoir temperature was  $T = 90$  mK, and the bias voltage was  $V = 1$  mV.

We set our frequency scale so that  $\tilde{\omega} = 0$  corresponds to  $f_0$  and  $\tilde{\omega} = \pm 1$  corresponds to the fundamental harmonic frequency of the substrate oscillator bending mode ( $f_b = 580$  kHz), with subsequent integers corresponding to higher harmonics. In the experiment, the forward bias which causes electrons to tunnel from the left reservoir to the right reservoir is large enough that electron tunneling in the opposite direction, from right to left, is insignificant. Our calculations also confirm that the right-to-left tunneling amplitudes is nearly zero.

The theoretical noise calculation matches the experimental data (Figure 2(c) in Ref.<sup>2</sup>) very well. The calculation reproduces the correct position of the noise peaks and the magnitudes of the noise floor. The peak at  $\tilde{\omega} = 0$  is due to the fluctuation of the electron current  $\langle n \rangle$  in the

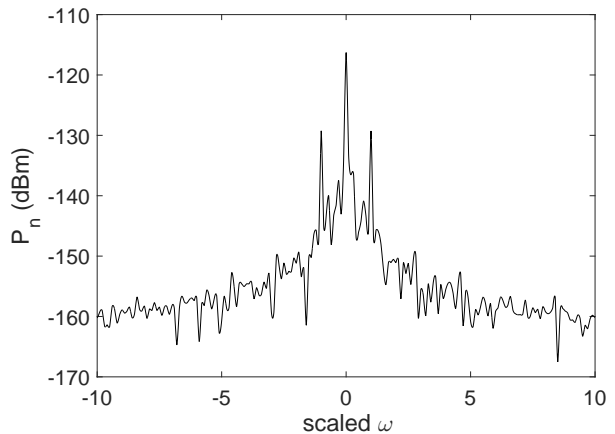


FIG. 2: Noise power spectrum as a function of dimensionless frequency. The temperature 90mK, circuit resonant frequency  $f_0 = 800$  MHz, applied voltage  $V = 1$  mV, tunneling amplitudes  $\tilde{\tau}_0 = 4 \times 10^{-2}$  and  $\tilde{\tau}_1 = 5 \times 10^{-5}$ , and phase shift  $\eta = \pi/2$  are chosen to simulate the experiment in Ref.<sup>2</sup>.

LC circuit. The peaks at  $\tilde{\omega} = \pm 1$  indicate that the QPC is coupled to the fundamental harmonic of the bending mode of the oscillator. Our analysis of each current fluctuation term in Eq. (14) reveals that the major contribution to the coupling noise comes from the noise terms  $\tilde{N}_x(x, t)$  and  $\tilde{N}_p(p, t)$ , which are associated with the position and momentum fluctuations, respectively, and their contributions are comparable.

The position and momentum fluctuations are connected through backaction via the correlation  $\langle \langle \{x, p\} n \rangle \rangle$  contained in  $\tilde{N}_{xp}(x, p, t)$ . Although the fluctuation amplitude of  $\tilde{N}_{xp}(x, p, t)$  is only about 1/1000 as large as the position and momentum fluctuation amplitudes, the backaction itself has a large role in transmitting the “kicks” between the position and momentum fluctuations, amplifying both fluctuation amplitudes. We can see this quantitatively: if the backaction is absent ( $\tilde{N}_{xp}(x, p, t) = 0$ ), both  $\tilde{N}_x(x, t)$  and  $\tilde{N}_p(p, t)$  dramatically decrease and the overall noise floor becomes 20 dBm lower than it would be with  $\tilde{N}_{xp}(x, p, t)$  present.

#### B. Position or momentum coupling?

The central role of the backaction raises the question whether the QPC is coupled to the substrate oscillator through position coupling or momentum coupling. Most researchers take the coupling between electronic devices and mechanical oscillators to be position-based, and we have adopted this assumption up to now in our analysis of the QPC-substrate coupling.

The dramatic decrease in both position and momentum fluctuations in the absence of backaction as seen in Sec. III A indicates that the backaction term acts as a channel between position and momentum, and transmits

every kick (backaction) from one to the other. Therefore, we now hypothesize that the type of coupling —position or momentum— will not affect the total amount of noise fluctuations, provided the backaction is included in the calculations and the system is given sufficient time to respond to the position and momentum’s mutual kicks, so that both position and momentum influence is fully incorporated into the system dynamics.

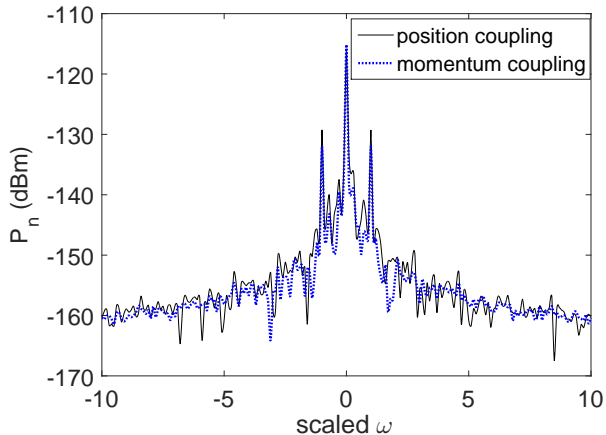


FIG. 3: Power spectrum of the position coupling (blue dotted line) and the momentum coupling (black solid line) as a function of dimensionless frequency. The parameters used are the same as those in Fig. 2.

To examine this hypothesis, we change the position coupling contained in  $T(x; t)$  to momentum coupling by replacing  $x/x_0$  with  $p/p_0$  in Eq. (A6) in Appx. A. Then, we re-derive the equation of motion and expressions for the currents, and evaluate the power noise spectrum. The resulting noise spectra are shown in Fig. 3. The peak noise heights, the widths of the peaks, and the magnitudes of noise floors are almost identical for both position and momentum coupling. This result highlights again the importance of backaction and shows the two couplings to be equivalent in terms of observable fluctuation noise. Note that our analyses pertain only to noise fluctuations. We make no claims about the equivalence of the two couplings schemes with respect to other transport quantities or the transient dynamics. We emphasize again that the position coupling in our model is a harmonic coupling. Anharmonic coupling, while potentially interesting, is beyond the scope of this paper.

### C. Information loss in the Markovian approximation

Finally, we examine the applicability of the Markovian approximation. As stated before, the Markovian approximation assumes that the system has a short memory meaning that the correlation time of electrons in the reservoirs is shorter than the coherence time between the

substrate oscillator and the electrons. On this assumption, many time-dependent tunneling coefficient terms (such as  $\xi$ ,  $D$ ,  $\gamma$ , in Appendix A) become zero or negligible. These simplifications make the tunneling parameters time-independent, and enables the equations to be solved analytically. However, in the Markovian approximation,  $\tilde{N}_{xp}$  is almost zero ( $\tilde{N}_{xp}$  is a factor of  $10^{-10}$  smaller than that of non-Markovian) even if the backaction term is included. As a result, the Markov approximation largely underestimates the noise in all terms of Eq. (14).

Figure 4 shows the power noise spectra for both the full non-Markovian evaluation and the Markovian approximation. The non-Markovian calculation is done numerically, while the Markovian calculation is done analytically. Both spectra show the LC circuit resonant frequency and the first harmonic of the substrate oscillator bending mode coupling as noise peaks. On the other hand, the amplitude of the noise floor in the Markovian approximation is about 45 dBm lower than in the full non-Markovian calculation.

Part of this gap comes from backaction, which is negligible in the Markovian approximation and, as shown in Sec. III A, contributes about 20 dBm to the noise floor. Other factors such as shot noise also contribute to the noise floor, which the Markovian approximation again severely underestimates by another  $\sim 25$  dBm.

Another difference between the Markovian and non-Markovian calculations is that the noise peaks in the Markovian approximation are very sharp spikes, whereas in the full non-Markovian calculation, the peaks are not as sharp and tall, but rather are broadened around the resonant frequencies.

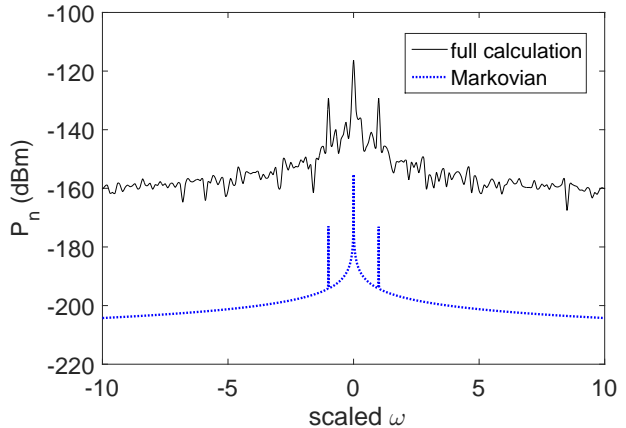


FIG. 4: Noise power spectrum as a function of dimensionless frequency. Comparing the Markov approximation (blue dotted line) to the full non-Markovian approximation (black solid line). The parameters used are the same as those in Fig. 2.

The Fano factor is the ratio of total noise to current noise as a function of the dimensionless frequency. Physically, the Fano factor is a good indicator of the strength

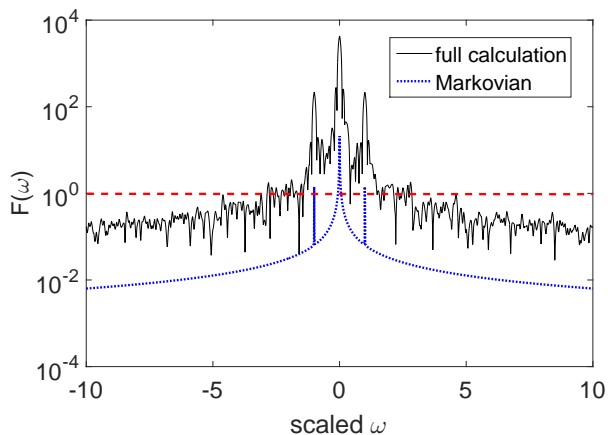


FIG. 5: Fano factor as a function of scaled frequency for both Markovian (blue dotted line) and non-Markovian approximation (black solid line) cases. The parameters used are the same as those in Fig. 4.  $F = 1$  (red dashed line) corresponds to a Poisson process.  $F > 1000$  is regarded as super-Poisson.

of the coupling between the electrons and the oscillator. Figure 5 shows Fano factors for both the Markovian approximation and full non-Markovian calculations. The noise reaches the super-Poisson range ( $> 1000$ ) in both the experiment and full calculation, but not in the Markovian approximation. This, too, contributes to the Markovian approximation's underestimating overall noise.

We see, then, that a simple Markovian approximation calculation suffices to demonstrate the existence and significance of the coupling of tunneling devices to substrates, since the noise peaks due to this coupling are clearly visible even in the Markovian plot. However, if one theoretically tries to explore a possibility to reduce the noise to increase the sensitivity of a QPC sensor, or to analyze a new device that takes an advantage of this extra mechanical degree of freedom in the future, then, the full numerical non-Markovian calculation is necessary.

#### IV. CONCLUSION

We have modeled electron transport and its noise spectrum for a tunnel junction device coupled to a substrate that acts as a mechanical oscillator. We focused on a QPC, so as to compare with available experimental data. In the first place, we made the standard assumption that the QPC and the substrate are coupled through position. In addition, we included backaction in our model. We obtained the noise spectrum from a full numerical evaluation, without making the Markovian approximation. We found that the current noise is strongly modified by the mechanical degrees of freedom. There are sharp peaks around the fundamental harmonic frequency of the substrate bending mode, and the noise floor is in-

creased. Our results reproduce all key features of the experimental results of Ref.<sup>2</sup>. Next we examined the nature of coupling. We calculated the noise spectrum for both position coupling and momentum coupling and found that the choice of coupling scheme does not make a difference in the noise spectrum as long as backaction is included and the noise spectra are evaluated in the steady state. The backaction acts as a channel between position and momentum influencing each other and amplify the fluctuations. Finally, we investigated the validity of the Markovian approximation. We compared the Markovian approximation with the full numerical result. While the Markovian approximation still shows key features, such as the fundamental resonance mode noise spike, it loses some important features, such as super-Poisson noise, noise peak broadening, and the noise floor. The Markovian approximation underestimate the effect of backaction, as well as other quantum noise, such as shot noise.

#### Acknowledgments

We thank Andreas Metz and Jonathan Tannenhauser for useful discussions.

#### Appendix A: $n$ -resolved master equation

The Hamiltonian of the system is

$$H_{tot} = H_{osc} + H_{res} + H_{int}, \quad (A1)$$

where  $H_{osc}$  and  $H_{res}$  are the non-interacting Hamiltonians for the substrate and the electron reservoirs. The objective here is to derive the master equation Eq. (8) in the main text.

We use the interaction picture and which represents our specific system from the general, time local, non-Markovian master equation Eq. (6).

$$\frac{d}{dt}\rho_{osc}(t) = -\frac{1}{\hbar^2} \int_0^t dt' Tr_{res} [H_{int}(t), [H_{int}(t'), \rho_{osc}(t) \otimes \rho_{res}]], \quad (A2)$$

where the interaction Hamiltonian,  $H_{int}$ , describes the tunneling electrons that are coupled to the substrate, and is given by

$$H_{int} = T(x; t) \sum_{k,q} Y^\dagger a_{R,k}^\dagger a_{L,q} + H.c.. \quad (A3)$$

We employ a charge counting method mentioned in the main text, which count the tunneling electrons  $n$  from the left reservoir to the right reservoir through the tunneling junction. The dimensionless charge counting operators

$\hat{Y}$  and  $\hat{Y}^\dagger$  are defined as

$$\hat{Y}\rho(n;t) \equiv \rho(n+1;t)(t), \quad (\text{A4})$$

$$\hat{Y}^\dagger\rho(n;t) \equiv \rho(n-1;t)(t). \quad (\text{A5})$$

The oscillator-position dependent tunneling amplitude of electrons  $T(x;t)$  is

$$T(x,t) = \frac{1}{\Lambda} \left( \tilde{\tau}_0 + e^{i\eta\tilde{\tau}_1} \frac{x(t)}{x_0} \right), \quad (\text{A6})$$

and

$$x(t) = x \cos \omega_0 t + \frac{p}{M\omega_0} \sin \omega_0 t, \quad (\text{A7})$$

where  $\Lambda = \Lambda(\epsilon_{L,q}, \epsilon_{R,k})$  is the density of states and a function of the energy of the electrons in the left,  $\epsilon_{L,q}$ , and right  $\epsilon_{R,k}$ , reservoirs.  $\tilde{\tau}_0$  and  $\tilde{\tau}_1$  are the dimensionless tunneling amplitudes without and with the vibration mode coupling, respectively.  $\eta$  is the phase difference between the  $\tilde{\tau}_0$  and  $\tilde{\tau}_1$ , and  $x_0 = \sqrt{\hbar/2M\omega_0}$ , where  $M$  and  $\omega_0$  are the mass and the resonant frequency of the substrate oscillator, respectively. A rough value of  $\tilde{\tau}_1$  is obtained from the coupling coefficient  $\lambda$ , which is geometry and material dependent and calculated in Ref.<sup>2</sup> using the experimental values. We take this  $\lambda$  and convert to dimensionless tunneling amplitude  $\tilde{\tau}_1 \approx 10^{-5}$ .  $\tilde{\tau}_0$  is set to  $\tilde{\tau}_0 \approx 10^{-2} \sim 10^{-121,22}$ . Then we finely tune these coefficients numerically.

We note that the tunneling amplitude in Eq. (A6) is linear on the position. This model is valid for the weak coupling which allows us to use the linear response theory. We also need the temperature range where the energy cost to add a charge  $e$  is larger than the thermal energy,  $k_{BT}$ . The model is applicable to wide variety of electronic devices including tunnel junctions, superconducting SET, and quantum dots. Smirnov et al<sup>32</sup>, considered an exponential coupling to the position to extend an applicability to arbitrary voltage applied to the junction and arbitrary temperature of electrons in leads.

Next, we want to find  $\langle n|Q|n \rangle$ , where  $Q$  is the integrand in Eq. (A2). For convenience, we group the operators  $T$  and  $Y$  as

$$j(x,t) \equiv T(x,t)Y^\dagger. \quad (\text{A8})$$

Inserting Eq. (A3) into  $Q$ , and tracing out the reservoir part result in

$$\begin{aligned} & \langle n|Q|n \rangle \\ &= [j(t)j^\dagger(t')\rho_{osc}(n,t) - j^\dagger(t')\rho_{osc}(n+1,t)j(t)] \\ & \times f_R(1-f_L)e^{-\frac{i}{\hbar}(\epsilon_L-\epsilon_R)(t-t')} \\ &+ [\rho_{osc}(n,t)j(t')j^\dagger(t) - j^\dagger(t)\rho_{osc}(n+1,t)j(t')] \\ & \times f_R(1-f_L)e^{\frac{i}{\hbar}(\epsilon_L-\epsilon_R)(t-t')} \\ &+ [j^\dagger(t)j(t')\rho_{osc}(n,t) - j(t')\rho_{osc}(n-1,t)j^\dagger(t)] \\ & \times f_L(1-f_R)e^{\frac{i}{\hbar}(\epsilon_L-\epsilon_R)(t-t')} \\ &+ [\rho_{osc}(n,t)j^\dagger(t')j(t) - j(t)\rho_{osc}(n-1,t)j^\dagger(t')] \\ & \times f_L(1-f_R)e^{-\frac{i}{\hbar}(\epsilon_L-\epsilon_R)(t-t')}. \end{aligned} \quad (\text{A9})$$

As the reservoirs are in equilibrium, we have the following electron correlation functions

$$\begin{aligned} & \langle a_L^\dagger(t)a_R(t) \rangle = 0, \\ & \langle a_L^\dagger(t)a_{L'}(t') \rangle = f_{LL'}\delta_{LL'}, \\ & \langle a_{L(R)}^\dagger(t')a_{L(R)}(t) \rangle = f_{L(R)} - 1 \\ & \langle a_\alpha^\dagger a_\gamma a_\beta^\dagger a_\delta \rangle = \langle a_\alpha^\dagger a_\gamma \rangle \langle a_\beta^\dagger a_\delta \rangle - \langle a_\alpha^\dagger a_\delta \rangle \langle a_\beta^\dagger a_\gamma \rangle, \end{aligned} \quad (\text{A10})$$

with  $\alpha, \beta, \gamma, \delta = L, R$  and The last equation comes from the Wick's theorem.  $f_{L(R)}$  is the Fermi distribution function for the left (right) electron reservoir:

$$f_{L(R)} = \frac{1}{\exp[(\epsilon_{L(R)} - \mu_{L(R)})/k_B T] + 1}, \quad (\text{A11})$$

where  $\mu_{L(R)}$  is the chemical potential of the left (right) reservoirs,  $k_B$  is the Boltzmann constant and  $T$  is the reservoir temperature.

Equation (A9) is unfortunately not useful for actual evaluations since solving for all  $n$  numerically is impractical due to  $n$  being large. Thus, we take the counting field approach that transforms the sum of the number to a continuous field<sup>26</sup>. The number  $n$  is transformed to the counting field  $\chi$  as

$$\rho_{osc}(\chi;t) = \sum_n e^{i\chi n} \rho_{osc}(n;t), \quad (\text{A12})$$

and its inverse-transform is

$$\sum_n e^{i\chi n} \rho_{osc}(n+\sigma,t) = e^{-i\chi\sigma} \rho_{osc}(\chi;t), \quad (\text{A13})$$

where  $\rho_{osc}(\chi,t)$  is the characteristic function describing the charge transfer events and  $\sigma = \pm 1$ . We define that  $\sigma = +1$  means the charge transfer from the left to the right reservoir (forward bias) and  $\sigma = -1$  from the right to the left reservoir (backward bias).

Transforming Eqs. (A2) and (A9) using Eq. (A12) and regrouping terms result in the counting field equivalent of the number-resolved ( $n$ -resolved) master equation

$$\frac{d}{dt}\rho_{osc}(\chi;t) = -\frac{1}{\hbar^2} \sum_{k,q} \frac{1}{\Lambda^2} \int_0^t dt' [U(\chi,t,t') + V(\chi,t,t')], \quad (\text{A14})$$

where  $\Lambda$  is the density of states for the electrons in the reservoirs, which was originally contained in the tunneling amplitude matrix  $T$ . The functions  $U$  and  $V$  contain the tunneling counting information and the two-time reservoir correlation functions. They also depend on the energy of tunneling junction of the QPC. The

terms  $U(\chi, t, t')$  and  $V(\chi, t, t')$  are given by

$$\begin{aligned}
U(\chi, t, t') &= [j(t)j^\dagger(t')\rho_{osc}(\chi) - e^{-i\chi}j^\dagger(t')\rho_{osc}(\chi)j(t) \\
&\quad + \rho_{osc}(\chi)j^\dagger(t')j(t) - e^{i\chi}j(t)\rho_{osc}(\chi)j^\dagger(t')] \\
&\quad \times F_s(t, t') \\
&\quad + [j(t)j^\dagger(t')\rho_{osc}(\chi) - e^{-i\chi}j^\dagger(t')\rho_{osc}(\chi)j(t) \\
&\quad - \rho_{osc}(\chi)j^\dagger(t')j(t) + e^{i\chi}j(t)\rho_{osc}(\chi)j^\dagger(t')] \\
&\quad \times F_a(t, t'), \tag{A15}
\end{aligned}$$

and

$$\begin{aligned}
V(\chi, t, t') &= [\rho_{osc}(\chi)j(t')j^\dagger(t) - e^{-i\chi}j^\dagger(t)\rho_{osc}(\chi)j(t') \\
&\quad + j^\dagger(t)j(t')\rho_{osc}(\chi) - e^{i\chi}j(t')\rho_{osc}(\chi)j^\dagger(t)] \\
&\quad \times F_s^\dagger(t, t') \tag{A16}
\end{aligned}$$

$$\begin{aligned}
&\quad + \rho_{osc}(\chi)j(t')j^\dagger(t) - e^{-i\chi}j^\dagger(t)\rho_{osc}(\chi)j(t') \\
&\quad - j^\dagger(t)j(t')\rho_{osc}(\chi) + e^{i\chi}j(t')\rho_{osc}(\chi)j^\dagger(t)] \\
&\quad \times F_a^\dagger(t, t'), \tag{A17}
\end{aligned}$$

with  $\rho_{osc} = (\chi)\rho_{osc}(\chi, t)$ .  $F_s$  and  $F_a$  are the symmetric and anti-symmetric two time reservoir correlation functions, respectively,

$$F_s(t, t') = \frac{1}{2} [f_L(1 - f_R) + f_R(1 - f_L)] e^{-\frac{i}{\hbar}(\epsilon_L - \epsilon_R)(t - t')}, \tag{A18}$$

$$F_a(t, t') = \frac{1}{2} [f_L(1 - f_R) - f_R(1 - f_L)] e^{-\frac{i}{\hbar}(\epsilon_L - \epsilon_R)(t - t')}. \tag{A19}$$

Using Eqs. (A14), (A15), and (A17), we regroup, perform some algebraic manipulations, and simplify and finally obtain

$$\begin{aligned}
\frac{d}{dt}\rho_{osc}(\chi; t) &= -\frac{i}{\hbar} \left[ H_{osc} - \frac{F_1 x}{x_0} - \frac{F_2 p}{x_0 M \omega_0}, \rho_{osc}(\chi; t) \right] \\
&\quad - \frac{1}{\hbar^2} \sum_{k, q} \frac{1}{\Lambda^2} \int_0^t dt' [\alpha_s + \alpha_a + \beta_s + \beta_a], \tag{A20}
\end{aligned}$$

where  $F_1(\eta, t)$  and  $F_2(\eta, t)$  are backaction energies given by

$$F_{1(2)}(\eta, t) = 2\hbar \sin \eta \sum_{\sigma=\pm 1} \tilde{\tau}_0 \tilde{\tau}_1 \xi_{a, \sigma}^{+(-)}, \tag{A21}$$

with  $\xi_{a, \sigma}^{+(-)}$  the tunneling parameter with its full expression is found in Eq. (A34). The sum runs for all the energy modes available. The terms in the second line describe the dynamics of the oscillator coupled to the QPC. For brevity, we use short-hand notation  $\rho = \rho_{osc}(\chi, t)$ ,  $\alpha_s = \alpha_s(\chi, t, t')$ ,  $\alpha_a = \alpha_a(\chi, t, t')$ ,  $\beta_s = \beta_s(\chi, t, t')$  and  $\beta_a = \beta_a(\chi, t, t')$ . The subscripts  $s$  and  $a$  denote symmetric and antisymmetric functions, respectively. The full expression of each term is shown below.

$$\begin{aligned}
\alpha_s &= (2\rho\tilde{\tau}_0^2 + A_1 + A_2 + A_3 + A_4 + A_5 \\
&\quad + A_6 + A_7 + A_8 + A_9) F_s \tag{A22}
\end{aligned}$$

$$\begin{aligned}
&\quad - e^{-i\chi} (A_{10} + A_{11} + A_{12} + A_{13} + A_{14}) F_s \\
&\quad - e^{i\chi} (\rho\tilde{\tau}_0^2 + A_{15} + A_{16} + A_{17} + A_{18} + A_{19}) F_s \tag{A23}
\end{aligned}$$

$$\begin{aligned}
\alpha_a &= (B_1 + B_2 + B_3 + B_4 + B_5 + B_6 + B_7) F_a \\
&\quad - e^{-i\chi} (B_8 + B_9 + B_{10} + B_{11}) F_a \\
&\quad + e^{i\chi} (\rho\tilde{\tau}_0^2 + B_{12} + B_{13} + B_{14} + B_{15}) F_a \tag{A24}
\end{aligned}$$

$$\begin{aligned}
\beta_s &= (2\rho\tilde{\tau}_0^2 + C_1 + C_2 + C_3 + C_4 + C_5 \\
&\quad + C_6 + C_7 + C_8 + C_9) F_s^\dagger \tag{A25}
\end{aligned}$$

$$\begin{aligned}
&\quad - e^{-i\chi} (\rho\tilde{\tau}_0^2 + C_{10} + C_{11} + C_{12} + C_{13}) F_s^\dagger \\
&\quad - e^{i\chi} (\rho\tilde{\tau}_0^2 + C_{14} + C_{15} + C_{16} + C_{17}) F_s^\dagger, \tag{A26}
\end{aligned}$$

$$\begin{aligned}
\beta_a &= (D_1 + D_2 + D_3 + D_4 + D_5 \\
&\quad + D_6 + D_7 + D_8) F_a^\dagger \tag{A27}
\end{aligned}$$

$$\begin{aligned}
&\quad - e^{-i\chi} (\rho\tilde{\tau}_0^2 + D_9 + D_{10} + D_{11} + D_{12}) F_a^\dagger \\
&\quad + e^{i\chi} (\rho\tilde{\tau}_0^2 + D_{13} + D_{14} + D_{15} + D_{16}) F_a^\dagger. \tag{A28}
\end{aligned}$$

All terms from  $A_1$  to  $D_{16}$  are in Appx. C.

In the continuous limit, we substitute the sum to an integral over the energy (thus, over electron frequencies) of the left and the right reservoirs and write Eq. (A20) as

$$\begin{aligned}
\frac{d}{dt}\rho_{osc}(\chi, t) &= -\frac{i}{\hbar} [H_{osc} - F(\eta, t), \rho_{osc}(\chi, t)] \\
&\quad - \int_0^t dt' \int_0^\infty d\omega_{R, k} \int_0^\infty d\omega_{L, q} [\alpha_s + \beta_s + \alpha_a + \beta_a]. \tag{A29}
\end{aligned}$$

Evaluating the integrations in Eq. (A29), we finally obtain the form of the unconditional master equation that can be numerically evaluated to obtain the current and noise spectrum:

$$\frac{d}{dt}\rho_{osc}(t) = \varrho_0(\chi = 0, t) + \varrho_1(\chi, t), \tag{A30}$$

The full expressions for  $\varrho_0$  and  $\varrho_1(\chi, t)$  are:

$$\begin{aligned}
\varrho_0 = & -\frac{i}{\hbar} \left[ H_{osc} - \frac{F_1 x}{x_0} - \frac{F_2 p}{x_0 M \omega_0}, \rho \right] \\
& - \sum_{\sigma=\pm 1} \left\{ \frac{\tilde{\tau}_1^2}{x_0^2} ([x, [x, \rho]] D_{s,\sigma}^+ + [x^2, \rho] D_{a,\sigma}^+) \right. \\
& + \frac{\tilde{\tau}_1^2}{x_0^2 M \omega_0} \{ [x, [p, \rho]] \gamma_{s,\sigma}^+ + [x, \{p, \rho\}] \gamma_{a,\sigma}^+ \} \\
& + [p, \{x, \rho\}] D_{a,\sigma}^- + [p, [x, \rho]] D_{s,\sigma}^- \} \\
& \left. + \frac{\tilde{\tau}_1^2}{x_0^2 M^2 \omega_0^2} ([p^2, \rho] \gamma_{a,\sigma}^- + [p, [p, \rho]] \gamma_{s,\sigma}^-) \right\}, \quad (\text{A31})
\end{aligned}$$

$$\begin{aligned}
\varrho_1 = & - \sum_{\sigma=\pm 1} (1 - e^{-i\sigma\chi}) \\
& \left\{ 2\tilde{\tau}_0^2 \rho \xi_{s,\sigma} + \frac{\tilde{\tau}_0 \tilde{\tau}_1}{x_0} (x \rho e^{-i\sigma\eta} + \rho x e^{i\sigma\eta}) \xi_{s,\sigma}^+ \right. \\
& + \frac{\tilde{\tau}_0 \tilde{\tau}_1}{x_0 M \omega_0} (p \rho e^{-i\sigma\eta} + \rho p e^{i\sigma\eta}) \xi_{s,\sigma}^- \\
& + \frac{\tilde{\tau}_0 \tilde{\tau}_1}{x_0} (x \rho e^{-i\sigma\eta} - \rho x e^{i\sigma\eta}) \xi_{s,\sigma}^+ \\
& + \frac{\tilde{\tau}_0 \tilde{\tau}_1}{x_0 M \omega_0} (p \rho e^{-i\sigma\eta} - \rho p e^{i\sigma\eta}) \xi_{s,\sigma}^- \\
& + \frac{\tilde{\tau}_1^2}{x_0^2} \left( x \rho x D_{s,\sigma}^+ + p \rho p \frac{\gamma_{s,\sigma}^-}{M^2 \omega_0^2} \right) \\
& - \frac{\tilde{\tau}_1^2}{x_0^2 M \omega_0} (x \rho p - p \rho x) (\gamma_{a,\sigma}^+ - D_{a,\sigma}^-) \\
& \left. + \frac{\tilde{\tau}_1^2}{x_0^2 M \omega_0} (x \rho p + p \rho x) (\gamma_{s,\sigma}^+ + D_{s,\sigma}^-) \right\}, \quad (\text{A32})
\end{aligned}$$

where  $\rho = \rho_{osc}(t)$ ,  $x = x(t)$ ,  $p = p(t)$ , and  $\xi$ ,  $D$  and  $\gamma$  are the tunneling parameters given by

$$\xi_{s(a),\sigma}(t) = \Gamma_{s(a),\sigma} + \Gamma_{s(a),\sigma}^\dagger, \quad (\text{A33})$$

$$\begin{aligned}
\xi_{s(a),\sigma}^+(t) &= \cos \omega_0 t \xi_{s(a),\sigma}(t), \\
\xi_{s(a),\sigma}^-(t) &= \sin \omega_0 t \xi_{s(a),\sigma}(t), \quad (\text{A34})
\end{aligned}$$

$$\begin{aligned}
D_{a(s),\sigma}^+(t) &= \Gamma_{s(a),\sigma}(+\omega_0) + \Gamma_{s(a),\sigma}(-\omega_0) \\
& + \Gamma_{s(a),\sigma}^\dagger(+\omega_0) + \Gamma_{s(a),\sigma}^\dagger(-\omega_0), \quad (\text{A35})
\end{aligned}$$

$$\begin{aligned}
D_{a(s),\sigma}^-(t) &= -i [\Gamma_{s(a),\sigma}(+\omega_0) - \Gamma_{s(a),\sigma}(-\omega_0)] \\
& - i [\Gamma_{s(a),\sigma}^\dagger(+\omega_0) - \Gamma_{s(a),\sigma}^\dagger(-\omega_0)], \quad (\text{A36})
\end{aligned}$$

$$\begin{aligned}
\gamma_{s(a),\sigma}^+(t) &= -i D_{a(s),\sigma}^+(t), \\
\gamma_{s(a),\sigma}^-(t) &= -i D_{a(s),\sigma}^-(t), \quad (\text{A37})
\end{aligned}$$

with,

$$\begin{aligned}
& \Gamma_{s(a),\sigma}(\pm \omega_0) \\
& = \Gamma_{s(a),\sigma}(\Omega_{L,k} - \Omega_{R,q} + eV/\hbar \pm \omega_0, t) \quad (\text{A38}) \\
& = \frac{1}{2} \int_0^t dt' \int_0^\infty d\Omega_{R,k} \int_0^\infty d\Omega_{L,q} \mathcal{F}_{s(a),\sigma} \\
& \quad \times \exp[i\sigma(\omega_{L,k} - \omega_{R,q} \pm \omega_0)(t-t')],
\end{aligned}$$

where we define

$$\hbar\Omega_{L(R),q(k)} \equiv \hbar\omega_{L(R),q(k)} - \mu_{L(R)}, \quad (\text{A39})$$

and  $\mu_{L(R)}$  is the chemical potential of the left (right) reservoir, and

$$\mathcal{F}_{s(a)} = 2F_{s(a)} e^{\frac{i}{\hbar}(\epsilon_L - \epsilon_R)(t-t')}. \quad (\text{A40})$$

With the results above, all the transport properties of the system can be determined from the Eq. (A30) and using the formula

$$\begin{aligned}
& \frac{d}{dt} \langle x^{m_1} p^{m_2} n^{m_3}(t) \rangle \\
& = (i^{m_3}) \text{Tr}_{osc} \left[ x^{m_1} p^{m_2} \frac{\partial^{m_3}}{\partial \chi^{m_3}} \frac{d}{dt} \rho(\chi; t) \right]_{\chi=0}, \quad (\text{A41})
\end{aligned}$$

where  $m_i$ , is any integer moment number.

## Appendix B: Current and noise spectrum

### 1. Current

The average current is given by

$$\langle I(t) \rangle = 2e \frac{d}{dt} \langle n(t) \rangle, \quad (\text{B1})$$

where  $e$  is the electron charge,  $n$  is the number of transferred electrons across the junction at time  $t$ , and  $\langle n \rangle$  is given by

$$\frac{d}{dt} \langle n(t) \rangle = i \text{Tr}_{osc} \left[ \frac{d}{d\chi} \left( \frac{d}{dt} \rho_{osc}(\chi, t) \right) \right]_{\chi=0}, \quad (\text{B2})$$

where  $\frac{d}{dt} \rho_{osc}(\chi, t)$  is given by Eq. (8). Performing the calculations of Eq. (B2) and simplifying, we obtain

$$\frac{\langle I(t) \rangle}{2e} = \frac{1}{2e} \left( \langle I \rangle_0 + \langle I \rangle_x + \langle I \rangle_p + \langle I \rangle_{xp} + \langle I \rangle_q \right), \quad (\text{B3})$$

where physical interpretation of each term is explained in the main text. The current components are given by

$$\langle I(t) \rangle_0 = 2\tilde{\tau}_0^2 \xi_{s,\sigma}(t), \quad (\text{B4})$$

$$\begin{aligned}
\langle I(t) \rangle_x &= \langle \hat{x} \rangle \frac{2\tilde{\tau}_0 \tilde{\tau}_1}{x_0} \left[ \cos \eta \xi_{s,(+)}^+(t) - i \sin \eta \xi_{s,(+)}^+(t) \right] \\
& + \langle \hat{x}^2 \rangle \frac{\tilde{\tau}_1^2 D_{s,(+)}^+(t)}{x_0^2}, \quad (\text{B5})
\end{aligned}$$

$$\begin{aligned} \langle I(t) \rangle_{\text{p}} &= \langle \hat{p} \rangle \frac{2\tilde{\tau}_0\tilde{\tau}_1}{x_0 M \omega_0} \left[ \cos \eta \xi_{s,(+)}^-(t) - i \sin \eta \xi_{a,(+)}^-(t) \right] \\ &+ \langle \hat{p}^2 \rangle \frac{\tilde{\tau}_1^2 \gamma_{s,(+)}^-(t)}{x_0^2 M^2 \omega_0^2}, \end{aligned} \quad (\text{B6})$$

$$\langle I(t) \rangle_{\text{xp}} = \langle \{\hat{x}, \hat{p}\} \rangle \frac{1}{x_0^2 M \omega_0} \left( \gamma_{s,(+)}^+(t) + D_{s,(+)}^- \right), \quad (\text{B7})$$

and

$$\langle I(t) \rangle_{\text{q}} = \frac{2i\hbar\tilde{\tau}_1^2}{x_0^2 M \omega_0} \left( \gamma_{a,(+)}^+(t) - D_{a,(+)}^-(t) \right). \quad (\text{B8})$$

Here,  $\langle I \rangle_0$  is the current without the oscillator coupling,  $\langle I \rangle_{\text{x}}$  and  $\langle I \rangle_{\text{p}}$  are the currents modulated by the coupled oscillator through the oscillator's position and momentum coordinates, and  $\langle I \rangle_{\text{q}}$  is the quantum correction to the overall current. The terms  $\langle \hat{x} \rangle$ ,  $\langle \hat{p} \rangle$  etc. are evaluated by solving Eq. (8) using Eq. (A41).

## 2. Noise

The spectral density is

$$\langle S(\omega) \rangle = 2e^2 \omega \int_0^{t'} dt e^{i\omega t} \frac{d}{dt} \langle \langle n^2(t) \rangle \rangle, \quad (\text{B9})$$

and the covariance  $\langle \langle n^2(t) \rangle \rangle$  is calculated by

$$\frac{d}{dt} \langle \langle n^2(t) \rangle \rangle = \frac{d}{dt} \langle n^2(t) \rangle - 2 \langle n(t) \rangle \frac{d}{dt} \langle n(t) \rangle. \quad (\text{B10})$$

All higher moments and the correlations between oscillator coordinates and transferred charge  $n$  are calculated from the master equation [Eq. (A2)] and by using Eq. (A41). Performing the calculations and simplifying, we obtain the three noise quantities that depend on position and momentum of the oscillator,

$$\begin{aligned} \frac{d}{dt} \langle \langle n^2(t) \rangle \rangle &= \frac{d}{dt} \langle n(t) \rangle + \tilde{N}_{\text{x}}(x, t) + \tilde{N}_{\text{p}}(p, t) \\ &+ \tilde{N}_{\text{xp}}(x, p, t), \end{aligned} \quad (\text{B11})$$

where

$$\begin{aligned} \tilde{N}_{\text{x}}(\hat{x}, t) &= \langle \langle \hat{x} n(t) \rangle \rangle \frac{4\tilde{\tau}_0\tilde{\tau}_1}{x_0} \left[ \cos \eta \xi_{s,(+)}^+(t) - i \sin \eta \xi_{a,(+)}^+(t) \right] \\ &+ \langle \langle \hat{x}^2 n(t) \rangle \rangle \frac{2\tilde{\tau}_1^2}{x_0^2} D_{s,(+)}^+(t), \end{aligned} \quad (\text{B12})$$

$$\begin{aligned} \tilde{N}_{\text{p}}(\hat{p}, t) &= \langle \langle \hat{p} n(t) \rangle \rangle \frac{4\tilde{\tau}_0\tilde{\tau}_1}{x_0 M \omega_0} \left[ \cos \eta \xi_{s,(+)}^-(t) - i \sin \eta \xi_{a,(+)}^-(t) \right] \\ &+ \langle \langle \hat{p}^2 n(t) \rangle \rangle \frac{2\tilde{\tau}_1^2}{x_0^2 M^2 \omega_0^2} \gamma_{s,(+)}^-(t) \end{aligned} \quad (\text{B13})$$

$$\tilde{N}_{\text{xp}}(\hat{x}, \hat{p}, t) = \langle \langle \{\hat{x}, \hat{p}\} n(t) \rangle \rangle \frac{2\tilde{\tau}_1^2}{x_0^2 M \omega_0} \left( \gamma_{s,(+)}^+(t) + D_{s,(+)}^- \right) \quad (\text{B14})$$

Again, all correlations can be obtained by solving Eq. (A2) with Eq. (A41).

Finally, we note the dimensionless scaling used in this paper. The dimensionless frequency, temperature, applied bias voltage and time are given by

$$\tilde{\omega} = \frac{\omega}{\omega_0}, \quad \tilde{T} = \frac{k_B T}{\hbar \omega_0}, \quad \tilde{V} = \frac{eV}{\hbar \omega_0}, \quad \tilde{t} = \omega_0 t, \quad (\text{B15})$$

where  $V$  is the applied voltage. The dimensionless position and momentum operators of the oscillator are given by

$$\tilde{x} \equiv x \left( \frac{\hbar}{2M\omega_0} \right)^{-1/2}, \quad \tilde{p} \equiv p \left( \frac{\hbar M \omega_0}{2} \right)^{-1/2}. \quad (\text{B16})$$

## Appendix C: Details of the terms used in Appx. A

$$A_1 = (x\rho + \rho x) \frac{\tilde{\tau}_0\tilde{\tau}_1 e^{-i\eta} \cos \omega_0 t'}{x_0} \quad (\text{C1})$$

$$A_2 = (p\rho + \rho p) \frac{\tilde{\tau}_0\tilde{\tau}_1 e^{-i\eta} \sin \omega_0 t'}{x_0 M \omega_0} \quad (\text{C2})$$

$$A_3 = \left[ (x\rho + \rho x) \cos \omega_0 t + (p\rho + \rho p) \frac{\sin \omega_0 t}{M \omega_0} \right] \frac{\tilde{\tau}_0\tilde{\tau}_1 e^{i\eta}}{x_0} \quad (\text{C3})$$

$$A_4 = (px\rho + \rho xp) \frac{\tilde{\tau}_1^2 \sin \omega_0 t \cos \omega_0 t'}{x_0^2 M \omega_0} \quad (\text{C4})$$

$$A_5 = (p^2\rho + \rho p^2) \frac{\tilde{\tau}_1^2 \sin \omega_0 t \sin \omega_0 t'}{x_0^2 M^2 \omega_0^2} \quad (\text{C5})$$

$$A_6 = (x^2\rho - 2x\rho x + \rho x^2) \frac{\tilde{\tau}_1^2 \cos \omega_0 t \cos \omega_0 t'}{x_0^2} \quad (\text{C6})$$

$$A_7 = (xpp - xpp - p\rho x + \rho px) \cos \omega_0 t \sin \omega_0 t' \quad (\text{C7})$$

$$A_8 = 2x\rho x \frac{\tilde{\tau}_1^2 \cos \omega_0 t \cos \omega_0 t'}{x_0^2} \quad (\text{C8})$$

$$A_9 = (x\rho p + p\rho x) \frac{\tilde{\tau}_1^2 \cos \omega_0 t \sin \omega_0 t'}{x_0^2 M \omega_0} \quad (\text{C9})$$

$$A_{10} = \rho \tilde{\tau}_0^2 + x\rho \frac{\tilde{\tau}_0\tilde{\tau}_1 e^{-i\eta} \cos \omega_0 t'}{x_0} \quad (\text{C10})$$

$$A_{11} = p\rho \frac{\tilde{\tau}_0\tilde{\tau}_1 e^{-i\eta} \sin \omega_0 t'}{x_0 M \omega_0} \quad (\text{C11})$$

$$A_{12} = \rho x \frac{\tilde{\tau}_0 \tilde{\tau}_1 e^{i\eta} \cos \omega_0 t}{x_0} + \rho p \frac{\tilde{\tau}_0 \tilde{\tau}_1 e^{i\eta} \sin \omega_0 t}{x_0 M \omega_0} \quad (\text{C12})$$

$$A_{13} = \left( x \rho x \cos \omega_0 t + \frac{x \rho p}{M \omega_0} \sin \omega_0 t \right) \frac{\tilde{\tau}_1^2 \cos \omega_0 t'}{x_0^2} \quad (\text{C13})$$

$$A_{14} = \left( p \rho x \cos \omega_0 t + \frac{p \rho p}{M \omega_0} \sin \omega_0 t \right) \frac{\tilde{\tau}_1^2 \sin \omega_0 t'}{x_0^2 M \omega_0} \quad (\text{C14})$$

$$A_{15} = \rho x \frac{\tilde{\tau}_0 \tilde{\tau}_1 e^{-i\eta} \cos \omega_0 t'}{x_0} \quad (\text{C15})$$

$$A_{16} = \rho p \frac{\tilde{\tau}_0 \tilde{\tau}_1 e^{-i\eta} \sin \omega_0 t'}{x_0 M \omega_0} \quad (\text{C16})$$

$$A_{17} = x \rho \frac{\tilde{\tau}_0 \tilde{\tau}_1 e^{i\eta} \cos \omega_0 t}{x_0} \quad (\text{C17})$$

$$A_{18} = p \rho \frac{\tilde{\tau}_0 \tilde{\tau}_1 e^{i\eta} \sin \omega_0 t}{x_0 M \omega_0} \quad (\text{C18})$$

$$A_{19} = \left( x \rho x \cos \omega_0 t + \frac{p \rho x}{M \omega_0} \sin \omega_0 t \right) \frac{\tilde{\tau}_1^2 \cos \omega_0 t'}{x_0^2} \quad (\text{C19})$$

$$A_{20} = \left( x \rho p \cos \omega_0 t + \frac{p \rho p}{M \omega_0} \sin \omega_0 t \right) \frac{\tilde{\tau}_1^2 \sin \omega_0 t'}{x_0^2 M \omega_0} \quad (\text{C20})$$

$$B_1 = \left[ (x \rho - \rho x) \cos \omega_0 t' + (p \rho - \rho p) \frac{\sin \omega_0 t'}{M \omega_0} \right] \frac{\tilde{\tau}_0 \tilde{\tau}_1 e^{-i\eta}}{x_0} \quad (\text{C21})$$

$$B_2 = \left[ (x \rho - \rho x) \cos \omega_0 t + (p \rho - \rho p) \frac{\sin \omega_0 t}{M \omega_0} \right] \frac{\tilde{\tau}_0 \tilde{\tau}_1 e^{i\eta}}{x_0} \quad (\text{C22})$$

$$B_3 = (p x \rho - \rho x p) \frac{\tilde{\tau}_1^2 \sin \omega_0 t \cos \omega_0 t'}{x_0^2 M \omega_0} \quad (\text{C23})$$

$$B_4 = (p^2 \rho - \rho p^2) \frac{\tilde{\tau}_1^2 \sin \omega_0 t \sin \omega_0 t'}{x_0^2 M^2 \omega_0^2} \quad (\text{C24})$$

$$B_5 = (x^2 \rho - \rho x^2) \frac{\tilde{\tau}_1^2 \cos \omega_0 t \cos \omega_0 t'}{x_0^2} \quad (\text{C25})$$

$$B_6 = (p \rho x - x \rho p) \frac{\tilde{\tau}_1^2 \cos \omega_0 t \sin \omega_0 t'}{x_0^2 M \omega_0} \quad (\text{C26})$$

$$B_7 = (x p \rho + x \rho p - p \rho x - \rho p x) \frac{\tilde{\tau}_1^2 \cos \omega_0 t \sin \omega_0 t'}{x_0^2 M \omega_0} \quad (\text{C27})$$

$$B_8 = \rho \tilde{\tau}_0^2 + \left( x \rho \cos \omega_0 t' + p \rho \frac{\sin \omega_0 t'}{M \omega_0} \right) \frac{\tilde{\tau}_0 \tilde{\tau}_1 e^{-i\eta}}{x_0} \quad (\text{C28})$$

$$B_9 = \left( \rho x \cos \omega_0 t + \rho p \frac{\sin \omega_0 t}{M \omega_0} \right) \frac{\tilde{\tau}_0 \tilde{\tau}_1 e^{i\eta}}{x_0} \quad (\text{C29})$$

$$B_{10} = \left( x \rho x \cos \omega_0 t + x \rho p \frac{\sin \omega_0 t}{M \omega_0} \right) \frac{\tilde{\tau}_1^2 \cos \omega_0 t'}{x_0^2} \quad (\text{C30})$$

$$B_{11} = \left( p \rho x \cos \omega_0 t + p \rho p \frac{\sin \omega_0 t}{M \omega_0} \right) \frac{\tilde{\tau}_1^2 \sin \omega_0 t'}{x_0^2 M \omega_0} \quad (\text{C31})$$

$$B_{12} = \left( \rho x \cos \omega_0 t' + \rho p \frac{\sin \omega_0 t'}{M \omega_0} \right) \frac{\tilde{\tau}_0 \tilde{\tau}_1 e^{-i\eta}}{x_0} \quad (\text{C32})$$

$$B_{13} = \left( x \rho \cos \omega_0 t + p \rho \frac{\sin \omega_0 t}{M \omega_0} \right) \frac{\tilde{\tau}_0 \tilde{\tau}_1 e^{i\eta}}{x_0} \quad (\text{C33})$$

$$B_{14} = \left( x \rho x \cos \omega_0 t + p \rho x \frac{\sin \omega_0 t}{M \omega_0} \right) \frac{\tilde{\tau}_1^2 \cos \omega_0 t'}{x_0^2} \quad (\text{C34})$$

$$B_{15} = \left( x \rho p \cos \omega_0 t + p \rho p \frac{\sin \omega_0 t}{M \omega_0} \right) \frac{\tilde{\tau}_1^2 \sin \omega_0 t'}{x_0^2 M \omega_0} \quad (\text{C35})$$

$$C_1 = (x \rho + \rho x) \frac{\tilde{\tau}_0 \tilde{\tau}_1 e^{i\eta} \cos \omega_0 t'}{x_0} \quad (\text{C36})$$

$$C_2 = (p \rho + \rho p) \frac{\tilde{\tau}_0 \tilde{\tau}_1 e^{i\eta} \sin \omega_0 t'}{x_0 M \omega_0} \quad (\text{C37})$$

$$C_3 = \left[ (x \rho + \rho x) \cos \omega_0 t + (p \rho + \rho p) \frac{\sin \omega_0 t}{M \omega_0} \right] \frac{\tilde{\tau}_0 \tilde{\tau}_1 e^{-i\eta}}{x_0} \quad (\text{C38})$$

$$C_4 = (p x \rho + \rho x p) \frac{\tilde{\tau}_1^2 \sin \omega_0 t \cos \omega_0 t'}{x_0^2 M \omega_0} \quad (\text{C39})$$

$$C_5 = (p^2 \rho + \rho p^2) \frac{\tilde{\tau}_1^2 \sin \omega_0 t \sin \omega_0 t'}{x_0^2 M^2 \omega_0^2} \quad (\text{C40})$$

$$C_6 = (x^2 \rho - 2 x \rho x + \rho x^2) \frac{\tilde{\tau}_1^2 \cos \omega_0 t \cos \omega_0 t'}{x_0^2} \quad (\text{C41})$$

$$C_7 = (x p \rho - x \rho p - p \rho x + \rho p x) \frac{\tilde{\tau}_1^2 \cos \omega_0 t \sin \omega_0 t'}{x_0^2 M \omega_0} \quad (\text{C42})$$

$$C_8 = 2 x \rho x \frac{\tilde{\tau}_1^2 \cos \omega_0 t \cos \omega_0 t'}{x_0^2} \quad (\text{C43})$$

$$C_9 = (x\rho p + p\rho x) \frac{\tilde{\tau}_1^2 \cos \omega_0 t \sin \omega_0 t'}{x_0^2 M \omega_0} \quad (\text{C44})$$

$$C_{10} = \left( \rho x \cos \omega_0 t' + p\rho \frac{\sin \omega_0 t'}{M \omega_0} \right) \frac{\tilde{\tau}_0 \tilde{\tau}_1 e^{i\eta}}{x_0} \quad (\text{C45})$$

$$C_{11} = \left( x\rho \cos \omega_0 t + p\rho \frac{\sin \omega_0 t}{M \omega_0} \right) \frac{\tilde{\tau}_0 \tilde{\tau}_1 e^{-i\eta}}{x_0} \quad (\text{C46})$$

$$C_{12} = \left( x\rho x \cos \omega_0 t + p\rho x \frac{\sin \omega_0 t}{M \omega_0} \right) \frac{\tilde{\tau}_1^2 \cos \omega_0 t'}{x_0^2} \quad (\text{C47})$$

$$C_{13} = \left( x\rho p \cos \omega_0 t + p\rho p \frac{\sin \omega_0 t}{M \omega_0} \right) \frac{\tilde{\tau}_1^2 \sin \omega_0 t'}{x_0^2 M \omega_0} \quad (\text{C48})$$

$$C_{14} = \left( x\rho \cos \omega_0 t' + p\rho \frac{\sin \omega_0 t'}{M \omega_0} \right) \frac{\tilde{\tau}_0 \tilde{\tau}_1 e^{i\eta}}{x_0} \quad (\text{C49})$$

$$C_{15} = \left( \rho x \cos \omega_0 t + p\rho \frac{\sin \omega_0 t}{M \omega_0} \right) \frac{\tilde{\tau}_0 \tilde{\tau}_1 e^{-i\eta}}{x_0} \quad (\text{C50})$$

$$C_{16} = \left( x\rho x \cos \omega_0 t + x\rho p \frac{\sin \omega_0 t}{M \omega_0} \right) \frac{\tilde{\tau}_1^2 \cos \omega_0 t'}{x_0^2} \quad (\text{C51})$$

$$C_{17} = \left( p\rho x \cos \omega_0 t + p\rho p \frac{\sin \omega_0 t}{M \omega_0} \right) \frac{\tilde{\tau}_1^2 \sin \omega_0 t'}{x_0^2 M \omega_0} \quad (\text{C52})$$

$$D_1 = \left[ (x\rho - \rho x) \frac{\tilde{\tau}_0 \tilde{\tau}_1 e^{i\eta} \cos \omega_0 t'}{x_0} \right] \quad (\text{C53})$$

$$D_2 = (p\rho - \rho p) \frac{\tilde{\tau}_0 \tilde{\tau}_1 e^{i\eta} \sin \omega_0 t'}{x_0 M \omega_0} \quad (\text{C54})$$

$$D_3 = \left[ (x\rho - \rho x) \cos \omega_0 t + (p\rho - \rho p) \frac{\sin \omega_0 t}{M \omega_0} \right] \frac{\tilde{\tau}_0 \tilde{\tau}_1 e^{-i\eta}}{x_0} \quad (\text{C55})$$

$$D_4 = (p x \rho - \rho x p) \frac{\tilde{\tau}_1^2 \sin \omega_0 t \cos \omega_0 t'}{x_0^2 M \omega_0} \quad (\text{C56})$$

$$D_5 = (p^2 \rho - \rho p^2) \frac{\tilde{\tau}_1^2 \sin \omega_0 t \sin \omega_0 t'}{x_0^2 M^2 \omega_0^2} \quad (\text{C57})$$

$$D_6 = (x^2 \rho - \rho x^2) \frac{\tilde{\tau}_1^2 \cos \omega_0 t \cos \omega_0 t'}{x_0^2} \quad (\text{C58})$$

$$D_7 = (p\rho x - x\rho p) \frac{\tilde{\tau}_1^2 \cos \omega_0 t \sin \omega_0 t'}{x_0^2 M \omega_0} \quad (\text{C59})$$

$$D_8 = (x p \rho + x \rho p - p \rho x - \rho p x) \frac{\tilde{\tau}_1^2 \cos \omega_0 t \sin \omega_0 t'}{x_0^2 M \omega_0} \quad (\text{C60})$$

$$D_9 = \left( \rho x \cos \omega_0 t' + p\rho \frac{\sin \omega_0 t'}{M \omega_0} \right) \frac{\tilde{\tau}_0 \tilde{\tau}_1 e^{i\eta}}{x_0} \quad (\text{C61})$$

$$D_{10} = \left( x\rho \cos \omega_0 t + p\rho \frac{\sin \omega_0 t}{M \omega_0} \right) \frac{\tilde{\tau}_0 \tilde{\tau}_1 e^{-i\eta}}{x_0} \quad (\text{C62})$$

$$D_{11} = \left( x\rho x \cos \omega_0 t + p\rho x \frac{\sin \omega_0 t}{M \omega_0} \right) \frac{\tilde{\tau}_1^2 \cos \omega_0 t'}{x_0^2} \quad (\text{C63})$$

$$D_{12} = \left( x\rho p \cos \omega_0 t + p\rho p \frac{\sin \omega_0 t}{M \omega_0} \right) \frac{\tilde{\tau}_1^2 \sin \omega_0 t'}{x_0^2 M \omega_0} \quad (\text{C64})$$

$$D_{13} = \left( x\rho \cos \omega_0 t' + p\rho \frac{\sin \omega_0 t'}{M \omega_0} \right) \frac{\tilde{\tau}_0 \tilde{\tau}_1 e^{i\eta}}{x_0} \quad (\text{C65})$$

$$D_{14} = \left( \rho x \cos \omega_0 t + p\rho \frac{\sin \omega_0 t}{M \omega_0} \right) \frac{\tilde{\tau}_0 \tilde{\tau}_1 e^{-i\eta}}{x_0} \quad (\text{C66})$$

$$D_{15} = \left( x\rho x \cos \omega_0 t + p\rho x \frac{\sin \omega_0 t}{M \omega_0} \right) \frac{\tilde{\tau}_1^2 \cos \omega_0 t'}{x_0^2} \quad (\text{C67})$$

$$D_{16} = \left( x\rho p \cos \omega_0 t + p\rho p \frac{\sin \omega_0 t}{M \omega_0} \right) \frac{\tilde{\tau}_1^2 \sin \omega_0 t'}{x_0^2 M \omega_0} \quad (\text{C68})$$

<sup>1</sup> P.-W. Chen, C.-C. Jian and H.-S. Goan, Phys. Rev. B **83**, 115439 (2011).

<sup>2</sup> J. Stettenheim, M. Thalakulam, F. Pan, M. Bal, Z. Ji, W. Xue, L. Pfeiffer, K.W. West, M.P. Blencowe and A.J. Rimberg, Nature **466**, 09123 p86–90 (2010).

<sup>3</sup> S. H. Ouyang, J. Q. You and F. Nori, Phys. Rev. B **79**, 075304 (2009).

<sup>4</sup> L. F. Wei, Yu-xi Liu, C. P. Sun, and Franco Nori Phys. Rev. Lett. **97**, 237201 (2006).

<sup>5</sup> D. W. Utami, H.-S. Goan, and G. J. Milburn, Phys. Rev. B **70**, 075303 (2004).

<sup>6</sup> N. M. Chtchelkatchev, W. Belzig and C. Bruder, Phys. Rev. B **70**, 193305 (2004).

<sup>7</sup> Y. Zhang and M. P. Blencowe, J. Appl. Phys. **91**, 4249

- (2002).
- <sup>8</sup> A. Erbe, C. Weiss, W. Zwerger and R. H. Blick, Phys. Rev. Lett. **87**, 096106 (2001).
  - <sup>9</sup> H. G. Graighead, Science **290**, 1532 (2000).
  - <sup>10</sup> D. H. Santamore, Neill Lambert, Franco Nori, Phys. Rev. B **87**, 075422 (2013).
  - <sup>11</sup> A. D. Armour, Phys. Rev. B **70**, 165315 (2004).
  - <sup>12</sup> F. H. L. Koppens, C. Buizert, K. J. Tielrooij, I.T. Vink, K.C. Nowack, T. Meunier, L. P. Kouwenhoven and L. M. K. Vandersypen, Nature **442**, 766 (2006).
  - <sup>13</sup> D. V. Averin and E. V. Sukhorukov, Phys. Rev. Lett. **95**,126803 (2005).
  - <sup>14</sup> M. Pioro-Ladriere, R. Abolfath, P. Zawadzki, J. Lapointe, S. A. Studenikin, A. S. Sachrajda and P. Hawrylak, Phys. Rev. B **72**, 125307 (2005).
  - <sup>15</sup> J. R. Petta, A. C. Johnson, J. M. Taylor, E. A. Laird, A. Yacoby, M. D. Lukin, C. M. Marcus, M. P. Hanson and A. C. Gossard, Science **309**, 2180 (2005).
  - <sup>16</sup> S. Pilgram and M. Buttiker, Phys. Rev. Lett. **89**, 200401 (2002).
  - <sup>17</sup> J. Wabnig, D. V. Khomitsky, J. Rammer and A. L. Shelankov, Phys. Rev. B. **72** 165347 (2005).
  - <sup>18</sup> M. R. Geller and A. N. Cleland, Phys. Rev. A **71**, 032311 (2005).
  - <sup>19</sup> Y. Makhlin, G. Schon and A. Shnirman, Rev. Mod. Phys. **73**, 357 (2001).
  - <sup>20</sup> M. Poggio, M. P. Jura, C. L. Degen, M. A. Topinka, H. J. Mamin, D. Goldhaber-Gordon and D. Rugar, Nature Phys. **4**, 635 (2008).
  - <sup>21</sup> L. L. Benatov and M. P. Blencowe, Phys. Rev. B **86**, 075313 (2012).
  - <sup>22</sup> A. A. Clerk and S. M. Girvin, Phys. Rev. B **70**, 121303 (2004).
  - <sup>23</sup> A. Clerk, Phys. Rev. B **70**, 245306 (2004).
  - <sup>24</sup> J. Rammer, A. L. Shelankov and J. Wabnig Phys. Rev. B **70**,115327 (2004).
  - <sup>25</sup> S. D. Bennett and A. A. Clerk, Phys. Rev. B **78**, 165328 (2008).
  - <sup>26</sup> C. B. Doiron, B. Trauzettel and C. Bruder, Phys. Rev. B **76**, 195312 (2007).
  - <sup>27</sup> H. P. Breuer and F. Petruccione, *The Theory of Open Quantum Systems*, (Oxford University Press, Oxford U.K, 2002)
  - <sup>28</sup> D. K. C. MacDonald, Rep. Prog. Phys.,**12**, 56 (1949).
  - <sup>29</sup> S. Walter and B. Trauzettel, Phys. Rev. B **83**, 155411 (2011).
  - <sup>30</sup> H. Takahasi and M. Mori, Research Institute for Mathematical Science (RIMS), **9**, 721, (1974)
  - <sup>31</sup> T. Ooura and M. Mori., J. Comput. Appl. Math. **112**, 229 (1999).
  - <sup>32</sup> Anatoly Yu. Smirnov, Lev G. Mourokh, and Norman J. M. Horing, Phys. Rev. B **67**, 115312 (2003).